Characterization of thin poly(dimethylsiloxane)-based tissue-simulating phantoms with tunable reduced scattering and absorption coefficients at visible and near-infrared wavelengths

Gage J. Greening
Raeef Istfan
Laura M. Higgins
Kartik Balachandran
Darren Roblyer
Mark C. Pierce
Timothy J. Muldoon

Characterization of thin poly(dimethylsiloxane)-based tissue-simulating phantoms with tunable reduced scattering and absorption coefficients at visible and near-infrared wavelengths

Gage J. Greening,[a] **Raeef Istfan,**[b] **Laura M. Higgins,**[c] **Kartik Balachandran,**[a] **Darren Roblyer,**[b] **Mark C. Pierce,**[c] **and Timothy J. Muldoon**[a,*]
[a]University of Arkansas, Department of Biomedical Engineering, Fayetteville, Arkansas 72701, United States
[b]Boston University, Department of Biomedical Engineering, Boston, Massachusetts 02215, United States
[c]Rutgers, State University of New Jersey, Department of Biomedical Engineering, Piscataway, New Jersey 08854, United States

Abstract. Optical phantoms are used in the development of various imaging systems. For certain applications, the development of thin phantoms that simulate the physical size and optical properties of tissue is important. Here, we demonstrate a method for producing thin phantom layers with tunable optical properties using poly (dimethylsiloxane) (PDMS) as a substrate material. The thickness of each layer (between 115 and 880 μm) was controlled using a spin coater. The reduced scattering and absorption coefficients were controlled using titanium dioxide and alcohol–soluble nigrosin, respectively. These optical coefficients were quantified at six discrete wavelengths (591, 631, 659, 691, 731, and 851 nm) at varying concentrations of titanium dioxide and nigrosin using spatial frequency domain imaging. From the presented data, we provide lookup tables to determine the appropriate concentrations of scattering and absorbing agents to be used in the design of PDMS-based phantoms with specific optical coefficients. In addition, heterogeneous phantoms mimicking the layered features of certain tissue types may be fabricated from multiple stacked layers, each with custom optical properties. These thin, tunable PDMS optical phantoms can simulate many tissue types and have broad imaging calibration applications in endoscopy, diffuse optical spectroscopic imaging, and optical coherence tomography, etc. © The Authors.

1 Introduction

The translation of novel optical imaging techniques from a basic laboratory setting to a clinical setting requires substantial calibration and validation, which is often performed on tissue-simulating materials known as phantoms. Tissue-simulating phantoms have several broad applications in regard to imaging systems including optimizing software and hardware and the gathering of preclinical data in advance of clinical trials, and are necessary for providing proof of reproducibility between trials of certain optical imaging techniques.[1–4] For example, optical coherence tomography (OCT) may use phantoms to determine the vital instrumentation characteristics including axial and lateral resolutions and point spread function.[2,5–7] Diffuse optical spectroscopic imaging (DOSI) techniques may use phantoms for initial calibration and stability measurements between trials.[4] The features of phantoms that are viewed as especially important include precise control of phantom geometry, the ability to easily modify and quantify scattering and absorption properties across commonly used wavelengths, stability over time, a comparable refractive index to human tissue, and the ability to introduce thin layers of different optical properties to simulate heterogeneities commonly seen in tissue.[1,3,4,8,9]

These heterogeneities may represent layers of different cell types as seen in the interface between the dermis and epidermis of the skin, or malignant morphological changes in a single tissue type as a result of disease.[1]

When considering optical imaging techniques, a primary feature of phantom development is the control of optical properties (reduced scattering and absorption coefficients) to mimic human tissue.[2,9,10] Optical properties of myriad human tissues have previously been characterized and can provide a guideline for phantom design.[11] In addition, some applications are required to probe deep layers of tissues, such as the basement membrane or submucosa, which can exist up to 800 or more microns below the apical surface.[12,13] In such cases, modulation of the phantom geometry on the scale of tens to hundreds of microns is crucial in phantom development.[1,2,14–16] Therefore, the ability to reproducibly create thin tissue-like phantoms with tunable optical properties may be beneficial for a wide range of optical image techniques.[1,2,4,9,10]

Many other groups have attempted to address this need for their applications. Bruin et al. demonstrated a method to produce 50-μm thick phantoms by curing poly(dimethylsiloxane) (PDMS) between two glass plates. These phantoms contained either silicon or titanium dioxide as the scattering agent and ABS 551, a green dye, as the absorber.[1] Saager et al. demonstrated a method to produce 90-μm thick phantoms by curing PDMS in a custom well plate using titanium dioxide as the

scattering agent and either coffee, nigrosin, or India ink as the absorber.[3] Finally, Bae et al. demonstrated a method to use a spin coater to spin epoxy down to ultra-thin (5 μm) layers. India ink was used as the absorber.[15] Although these methods provided rigorous validation of tissue-simulating phantoms, all have specific limitations which we seek to address. Bruin et al. reported their optical properties only in terms of the attenuation coefficient (μ_t) instead of the more conventional reduced scattering (μ_s') and absorption (μ_a) coefficients commonly used to quantify tissue optical properties.[11] Saager et al. thoroughly reported on the wavelength dependence of their phantoms but did not provide information on the dependence of these optical properties on the concentrations of absorbing and scattering agents.[3] Finally, Bae et al. introduced a spin coating technique to produce ultra-thin layers. The resulting multilayered phantoms with included heterogeneities were permanent, meaning thin layers cannot be easily interchanged.[15] We seek to combine various aspects of the phantom design procedures briefly reviewed here to create unique tissue-simulating optical phantoms.[1,3,15]

We introduce a method to produce thin, interchangeable phantom layers with tunable optical properties using PDMS, an optically clear, silicone-based elastomer, simulating the epithelium.[9–12] PDMS was chosen because of its durability, optical stability over time, comparable refractive index to human tissue (1.4), and the easy manipulation of both layer thickness and optical properties through the addition of scattering and absorbing agents.[1,4,9]

Phantom thickness was controlled by spinning uncured PDMS on a clean, nonpatterned silicon wafer in a spin coater, in which the spin speed (100 to 1000 rpm) was manipulated to reproducibly create thin PDMS optical phantoms between 115 and 880 μm.[15,16] Thicker phantoms were constructed by pouring uncured PDMS into a mold. Preparing phantom layers in the range of 100 to 300 μm is especially important to model many tissue types, such as the skin, gingivae, esophagus, cervix, etc.[1,13,17–19]

Phantom optical properties were controlled by introducing varying concentrations of titanium dioxide and alcohol–soluble nigrosin as the scattering and absorbing agents, respectively.[1,9–12,20] The reduced scattering and absorption coefficients of PDMS-based phantoms with increasing concentrations of titanium dioxide and alcohol–soluble nigrosin were quantified by spatial frequency domain imaging (SFDI) at six discrete wavelengths (591, 631, 659, 691, 731, and 851 nm) across the visible to near-infrared spectrum.[21,22] Optical characterization with SFDI outside this wavelength range was unreliable. Based on the data presented here, lookup tables have been provided that list appropriate concentrations of titanium dioxide and alcohol–soluble nigrosin to use based on the desired reduced scattering and absorption coefficients. These lookup tables may be useful for researchers interested in developing similar phantoms for their specific imaging applications.

Once phantoms were characterized, individual thin phantom layers were stacked to create thicker, multilayer phantoms, which can model an optically heterogeneous tissue of interest.[3,7,14] Using SFDI, optical properties of multilayer phantoms were compared to single-layer phantoms with identical concentrations of titanium dioxide and alcohol–soluble nigrosin for validation. Furthermore, multilayered phantoms were imaged using OCT B-scanning for validation and qualitative purposes.

2 Materials and Methods

2.1 Design of Thin PDMS-Based Optical Phantom Layers for Characterization of Thickness

For each thin phantom, 6.5 ± 0.1 grams of PDMS (Sylgard 184 Silicone Elastomer Kit, Dow Corning, USA) elastomer base were dispensed into an ARE-100 conditioning mixer cup (Intertronics, UK). Next, the curing agent was dispensed into a 7-mL scintillation vial (VWR, USA) based on a 10:1 ratio of base to curing agent. Titanium dioxide (Sigma-Aldrich, USA) and alcohol–soluble nigrosin (Sigma-Aldrich, USA, SKU: 211680-25G) were used to control the reduced scattering coefficient (μ_s') and absorption coefficient (μ_a), respectively. Titanium dioxide (TiO$_2$) was weighed and dispensed into a 7-mL scintillation vial containing the curing agent. Next, a 1% w/v solution of nigrosin in ethanol was prepared and added to the scintillation vial. The mixture in the scintillation vial was mixed for 1 min on a vortex mixer (VWR, USA) to disperse large particles of TiO$_2$. Following this, the scintillation vial was placed in a Model 3510 sonicator (Branson Ultrasonics Corporation, USA) for 30 min to disperse small particles of TiO$_2$ and nigrosin emulsions in the curing agent solvent. The process of vortexing for 1 min and sonicating for 30 min was repeated a total of five times to ensure uniform scattering and absorption throughout.

The mixture of curing agent, TiO$_2$, and 1% w/v nigrosin/EtOH was then dispensed into a mixing cup containing the PDMS elastomer base. This final mixture was thoroughly mixed and degassed for three cycles in an ARE-100 conditioning mixer (Intertronics, UK) for a total of 12 min. Immediately following mixing and conditioning in the ARE-100 conditioning mixer, the uncured mixture was placed in an oven at 70°C for 3 min to initiate curing. The PDMS mixture was removed from the oven and slowly poured onto the center of a 10-cm silicon wafer (University Wafer, USA) within a G3P-8 spin coater (SCS Spin Coating Systems, USA).

The spin coater was optimized to accelerate to its peak speed in 4 s, spin at maximum speed for 20 s, and then decelerate to zero RPM in 4 s. Once the spin coater reached zero RPM, the silicon wafer, containing a thin film of partially cured PDMS mixture, was removed and placed in an oven at 70°C for 2 h to complete curing.

Thin phantoms were created at spin speeds of 100, 200, 300, 400, 500, 700, and 1000 rpm, with three trials of each. Each phantom at a particular spin coater speed was sampled six times for a total of 18 thickness measurements at each speed. Thickness was quantified by analyzing transmittance images of PDMS phantom layers. A transverse cut was made in each phantom and imaged using a wide-field microscope with a Nikon Plan Fluor 10X, 0.30 NA objective and Nikon DS-Fi2 camera. Calibration of the image scale was performed with a positive USAF 1951 resolution target. Images were analyzed using the MATLAB® Image Analysis Toolbox (Mathworks, USA).

2.2 Design of PDMS-Based Optical Phantoms for Characterization of Reduced Scattering and Absorption Coefficients

The μ_s' and μ_a of phantoms containing varying amounts of TiO$_2$ and 1% w/v nigrosin/EtOH were quantified with SFDI.[21,22] For analysis with SFDI, thicker phantoms (2.5 cm thick) were built using an ARE-100 conditioning mixer cup (Intertronics, UK) as

Table 1 Amounts of titanium dioxide (scattering agent) and nigrosin/ethanol solution (absorbing agent) per thick (2.5 cm) "semi-infinite" phantom quantified by spatial frequency domain imaging (SFDI).

Phantom number	TiO_2 (g/g)	1% w/v nigrosin/EtOH (μL/g)
1	0.001	0.5
2	0.002	0.5
3	0.003	0.5
4	0.004	0.5
5	0.005	0.5
6	0.006	0.5
7	0.007	0.5
8	0.008	0.5
9	0.001	1.0
10	0.001	2.0
11	0.001	3.0
12	0.001	4.0
13	0.001	5.0
14	0.001	7.0
15	0.001	10.0
16	0.001	40.0

a mold. Construction of thick phantoms followed the same procedure as the construction of thin phantoms up until the point the spin coater was introduced. Instead of using a spin coater to spin partially cured PDMS into a thin layer, completely mixed PDMS was placed in an oven at 70°C for 2 h to complete curing. Sixteen phantoms were created using this technique. Eight phantoms (#1–8 in Table 1) contained a constant amount of 1%
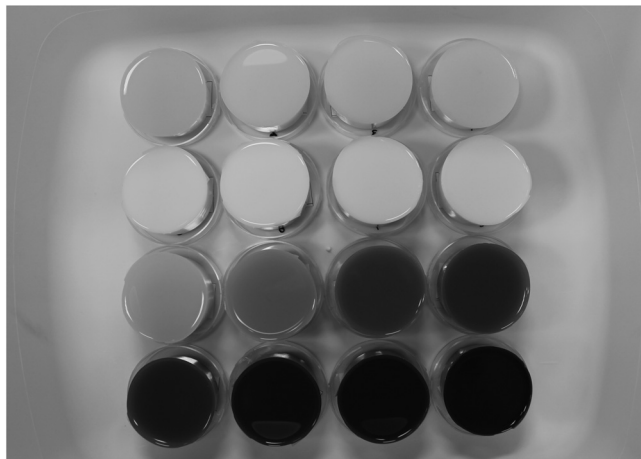
Fig. 1 Aerial view of the 16 phantoms used in the spatial frequency domain imaging (SFDI) characterization of μ_s' and μ_a, corresponding to Table 1. Phantoms used in this study are #1–4 (first row), #5–8 (second row), #9–12 (third row), and #13–16 (fourth row).

w/v nigrosin/EtOH solution with an increasing concentration of TiO_2 in a PDMS elastomer base to manipulate the μ_s'. Nine phantoms (#1 and 9–16 in Table 1) contained a constant amount of TiO_2 with an increasing concentration of 1% w/v nigrosin/EtOH solution in a PDMS elastomer base to manipulate the μ_a. As an example, 50 grams of PDMS elastomer base were used to create Phantom #5, 0.25 grams of TiO_2 and 25 μL of 1% w/v nigrosin/EtOH were added. Table 1 shows the breakdown of each phantom created for the quantification of optical properties by SFDI. In addition, Fig. 1 shows an aerial view of all 16 phantoms represented in Table 1.

2.3 Construction of Multilayer Phantoms for Inclusion of Heterogeneities

One multilayer phantom was constructed, quantified by SFDI, and compared to a single layer, "semi-infinite" control phantom with identical concentrations of optical agents.[21,22] The primary concern during construction of multilayer phantoms was the formation of air pockets between two adjacent layers. One possible technique to avoid air pocket formation was directly spinning uncured PDMS over an existing base layer to build multilayer tissue-simulating phantoms. While this method can successfully eliminate air pocket formation, it would not be suitable for creating thin layers that are easily interchangeable.[15] Instead, our method allowed for thin PDMS layers to readily be stacked and removed, creating diverse sets of multilayer phantoms for various optical imaging purposes. First, two 2.5-cm thick "semi-infinite" phantom layers were molded and cured in an ARE-100 conditioning mixer cup (Intertronics, UK), containing 0.002 g TiO_2 and 2.0 μL 1% w/v nigrosin/EtOH per gram PDMS elastomer base. Then, using the described spin coating method, two 200-μm layers were constructed, containing exactly the same concentrations of optical agents. After the two 200-μm layers finished curing, they were carefully peeled off the silicon wafer. Using a scapel, the layers were cut into approximately 3 cm² squares. Each thin-layer square was placed into a 70% ethanol/DI water solution and sonicated for 10 min to remove dust and other surface contaminants. Following this, two drops of ethanol were placed on one of the 2.5 cm "semi-infinite" base layers. One 200-μm layer was directly placed on top of the ethanol drops so that no visible air bubbles remained. This two-layer phantom was placed in an oven at 70°C for 3 min to allow evaporation of the ethanol, creating two adjacent layers without air pockets. These steps were repeated for the second 200-μm layer on the same multilayered phantom (Phantom #18 in Table 2). No thin layers were added to the second 2.5 cm "semi-infinite" base layer (Phantom #17 in Table 2). Table 2 shows the geometric specifications of the two phantoms.

Table 2 Thickness specifications for single- and multilayer control phantoms (for all layers: 0.002 g, TiO_2, and 2.0 μL 1% w/v nigrosin/EtOH in PDMS elastomer base).

Thickness (μm)	Phantom #17 (single layer)	Phantom #18 (multilayer)
Top layer	N/A	200
Middle layer	N/A	200
Bottom layer	25,000	25,000

Both phantoms were subjected to SFDI analysis to quantify μ_s' and μ_a at the six discrete wavelengths. This analysis served to validate the process of creating multilayer phantoms without air pocket formation. In addition, SFDI analysis on multilayered phantoms served to validate that thin (<880 μm) and thick (2.5 cm) phantoms layers with identical concentrations of optical agents have comparable optical properties. Because all layers contain identical concentrations of TiO$_2$ and 1% w/v nigrosin/EtOH, μ_s' and μ_a should be identical for both single-layer and multi-layer phantoms.

Additionally, one more three-layer multi-layer phantom was constructed and imaged using an OCT B-scan for qualitative purposes. First, one 2.5-cm thick phantom layer was molded and cured in an ARE-100 conditioning mixer cup (Intertronics, UK), containing 0.002 g titanium dioxide and 2.0 μL 1% w/v nigrosin/EtOH per g PDMS elastomer base. Then, using the described spin coating method, two 200-μm layers were constructed. The first 200-μm layer contained 0.006 g TiO$_2$ and 2.0 μL 1% w/v nigrosin/EtOH per g PDMS elastomer base, tripling the scattering agent concentration while keeping the absorbing agent concentration constant. The second 200-μm layer contained 0.002 g TiO$_2$ and 2.0 μL 1% w/v nigrosin/EtOH per g PDMS elastomer base (identical to the base layer). The first (optically different) thin layer was placed between the base layer and the second (optically identical) thin layer to produce a heterogeneous multilayer phantom that was imaged by an OCT B-scanning technique. These phantom images are compared to various types of human epithelium (skin and oral mucosa). Table 3 shows the geometric and optical specifications of the heterogeneous multilayer phantom for this comparative study using OCT. The OCT imaging was performed on a custom-built spectral-domain OCT platform with a center wavelength of 1325 nm, axial resolution of 8.0 μm (in air), lateral resolution of 22.5 μm, and maximum imaging depth of 3.0 mm (in air).[23] For phantom imaging, OCT cross-sections (B-scans) contained 500 A-lines acquired over a 5 mm scan width. B-scan images were generated by standard SD-OCT processing (spectrometer wavelength calibration, interpolation to evenly spaced samples in k-space, and Fourier transformation).[23] The OCT system used here operates at 1325 nm, further into the near-infrared range than our SFDI system was capable of testing (591 to 851 nm). The majority of the OCT imaging of tissues (including the epithelial tissues in which our phantoms seek to mimic) is done in the 1325-nm region.[23] Therefore, OCT B-scans were used for comparative purposes and not to characterize the optical properties of the phantoms.

Table 3 Thickness and optical concentration specifications for multilayer phantom imaged by an optical coherence tomography (OCT) B-scanning technique.

Phantom #19	Layer 1	Layer 2	Layer 3
Thickness (μm)	25,000	200	200
TiO$_2$ (g/g)	0.002	0.006	0.002
1 w/v% nigrosin/EtOH (μL/g)	2	2	2

3 Results

3.1 Characterization of Thickness of Thin PDMS-Based Optical Phantoms

Figure 2 shows the relationship between the primary, maximum 20-s spin speed and resulting thickness of the PDMS layers. Seven different spin speeds were used (100, 200, 300, 400, 500, 700, and 1000 rpm) to characterize the resulting thicknesses (between 115 and 880 μm) of thin PDMS-based phantoms.

3.2 Characterization of Reduced Scattering Coefficient of PDMS-Based Optical Phantoms

Figure 3 shows the relationship between the TiO$_2$ (scattering agent) in the PDMS elastomer base (g/g) and the resulting μ_s' (cm^{-1}) for six discrete wavelengths (nm) measured by SFDI (591, 621, 659, 691, 731, and 851 nm). Eight phantoms (#1–8 in Table 1) were used in this study which contained a constant amount of 1% w/v nigrosin/Et/OH (absorbing agent) and increasing concentrations of TiO$_2$ in a PDMS elastomer base (g/g).
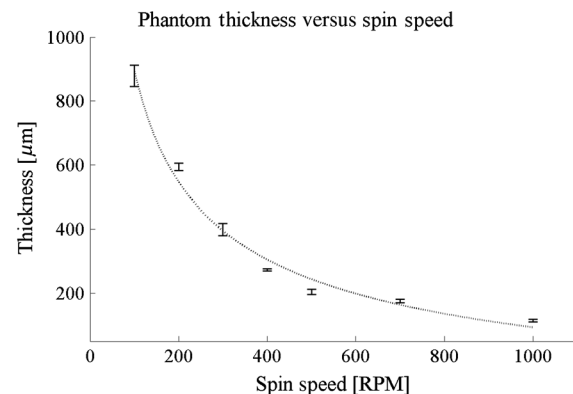
Fig. 2 Relationship between thickness of thin-layer phantoms and maximum 20-s spin speed of a spin coater. Here, phantoms were constructed between approximately 115 and 880 μm. The R^2 value for the curve of best fit is 0.988. Best fit lines were generated by the MATLAB curve-fitting toolbox (power fit).

Fig. 3 Relationship between μ_s' (cm^{-1}) and TiO$_2$ concentration in PDMS elastomer base (g/g) measured at six discrete wavelengths (591, 621, 659, 691, 731, and 851 nm) using SFDI analysis. Here, μ_s' values range between approximately 1 and 21 cm^{-1}. R^2 values for best fit lines from 591 to 851 nm are 0.994, 0.994, 0.994, 0.995, 0.995, and 0.998, respectively. Best fit lines were generated by the MATLAB curve-fitting toolbox (linear fit).

Fig. 4 Relationship between μ_s' (cm^{-1}) and 1% w/v nigrosin/EtOH concentrations in PDMS elastomer base (μL/g) measured at six discrete wavelengths (591, 621, 659, 691, 731, and 851 nm) using SFDI analysis. Best fit lines were generated by the MATLAB curve-fitting toolbox (linear fit).

In addition, μ_s' was measured at increasing 1% w/v nigrosin/EtOH concentrations in the PDMS elastomer base to determine if increasing the chosen absorbing agent would affect the bulk scattering properties. Figure 4 shows the relationship between 1 w/v% of nigrosin/EtOH concentration and the resulting μ_s' (cm^{-1}). Results from Phantom #16 are not shown in Fig. 4. The phantoms used in this experiment (#1, 9–15 in Table 1) all contained identical concentrations of the chosen scattering agent, TiO$_2$ (0.001 g/g).

3.3 Characterization of Absorption Coefficient of PDMS-Based Optical Phantoms

Figure 5 shows the relationship between 1 w/v% of the nigrosin/EtOH (absorbing agent) in a PDMS elastomer base (μL/g) and the resulting μ_a (cm^{-1}) for six discrete wavelengths measured by SFDI (591, 621, 659, 691, 731, and 851 nm). Nine phantoms (#1 and 9–16 in Table 1) were used in this study; they contained a constant amount of TiO$_2$ (scattering agent) and increasing 1% w/v nigrosin/EtOH concentrations in a PDMS elastomer base.

In addition, μ_a was measured at increasing TiO$_2$ concentrations in a PDMS elastomer base to determine if increasing the
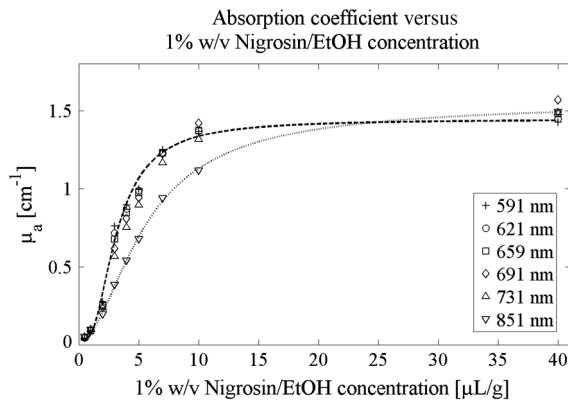
Fig. 5 Relationship between μ_a (cm^{-1}) and 1% w/v nigrosin/EtOH concentration in PDMS elastomer base (μL/g) measured at six discrete wavelengths (591, 621, 659, 691, 731, and 851 nm) using SFDI analysis. Here, absorption coefficients range between approximately 0 and 1.5 cm^{-1}. Best fit curves, generated by the MATLAB curve-fitting toolbox (power fit), are shown for the 591 nm (dashed) and 851 nm (dotted) wavelengths, respectively.
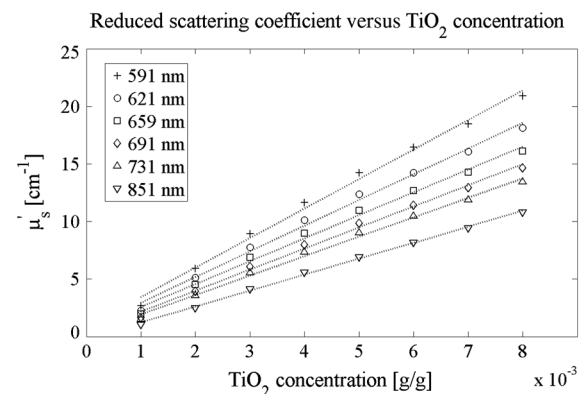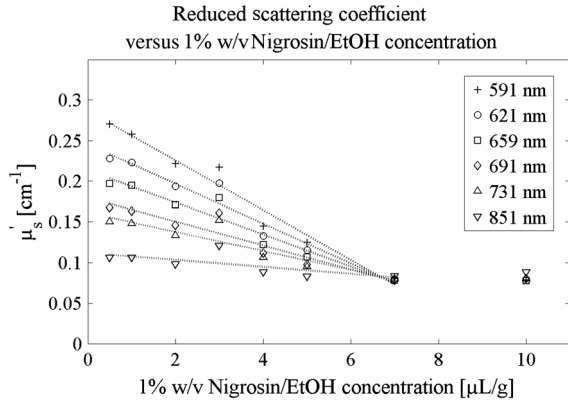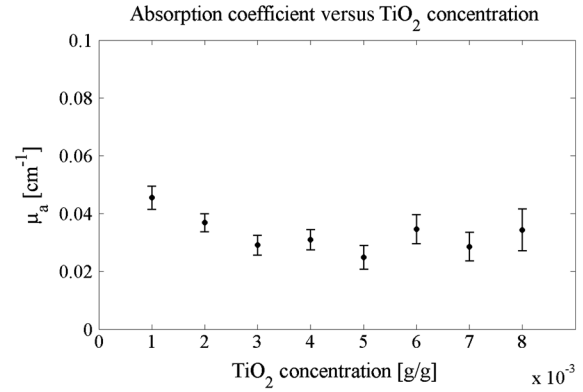

Fig. 6 Relationship between μ_a (cm^{-1}) and TiO$_2$ concentration in PDMS elastomer base (g/g) measured at six discrete wavelengths (591, 621, 659, 691, 731, and 851 nm) using SFDI analysis.

chosen scattering agent would affect the bulk absorbing properties. Figure 6 shows the relationship between TiO$_2$ concentration and the resulting μ_a (cm^{-1}). Eight phantoms (#1-8 in Table 1) were used in this study; they contained identical concentrations of the chosen absorbing agent, 1% w/v nigrosin/EtOH (0.5 μL/g).

3.4 Validation of Multilayer PDMS-Based Optical Phantoms

For the two phantoms specified in Table 2 (Phantoms # 17 and 18), μ_s' (cm^{-1}) and μ_a (cm^{-1}) were quantified with SFDI.[21,22] Phantom #17 (single-layer) consisted of only one thick 2.5-cm base layer, containing 0.002 g TiO$_2$ and 2.0 μL 1% w/v nigrosin/EtOH per gram PDMS elastomer base. Phantom #18 (multi-layer) consisted of one thick 2.5-cm base layer with two overlying 200-μm layers, all containing 0.002 g TiO$_2$ and 2.0 μL 1% w/v nigrosin/EtOH per gram PDMS elastomer base. This experiment attempted to validate the creation of multilayer phantoms by comparing the overall optical properties (μ_s' and μ_a) of single- and multi-layer phantoms with all layers containing identical concentrations of scattering and absorbing agents. Figure 7 shows the relationship between the wavelength and the resulting μ_s', while Fig. 8 shows the relationship between the wavelength and resulting μ_a for the single- (Phantom #17) and multi-layer (Phantom #18) phantoms specified in Table 2.
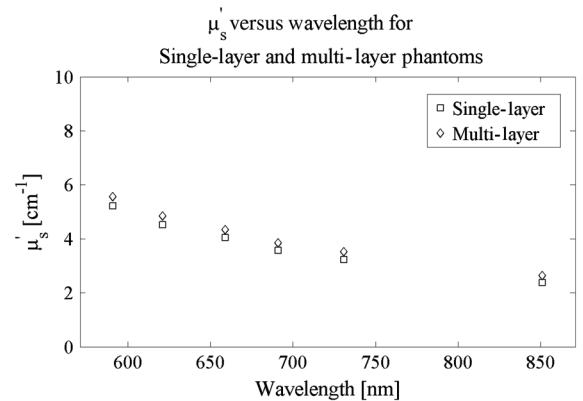
Fig. 7 Comparison of μ_s' (cm^{-1}) between a single-layer and a multi-layer phantom with identical concentrations of scattering and absorbing agents measured at six discrete wavelengths (591, 621, 659, 691, 731, and 851 nm) SFDI analysis. Average aggregate error was 7.7%.

μ_a versus wavelength for Single-layer and multi-layer phantoms
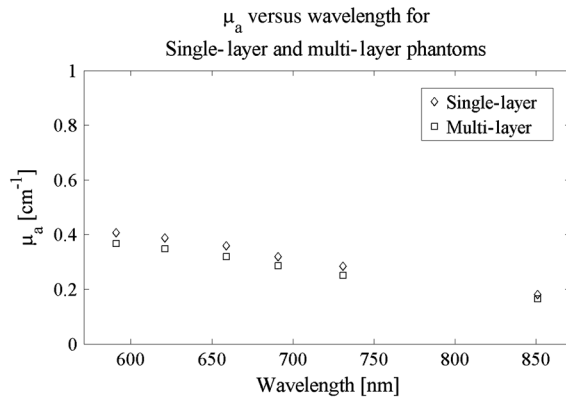
Fig. 8 Comparison of μ_a (cm^{-1}) between a single-layer and a multi-layer phantom with identical concentrations of scattering and absorbing agents measured at six discrete wavelengths (591, 621, 659, 691, 731, and 851 nm) using SFDI analysis. Average aggregate error was 10.9%.

Fig. 9 Images of multilayered PDMS-based phantoms compared to optical coherence tomography (OCT) B-scans of various human epithelium. (a) OCT B-scan of a three-layer phantom. Thickness in layers 1 and 2 (L1 and L2) was approximately 200 μm, respectively. TiO$_2$ concentration in layers 1, 2, and 3 (L3) were 0.002, 0.006, and 0.002 (g/g), re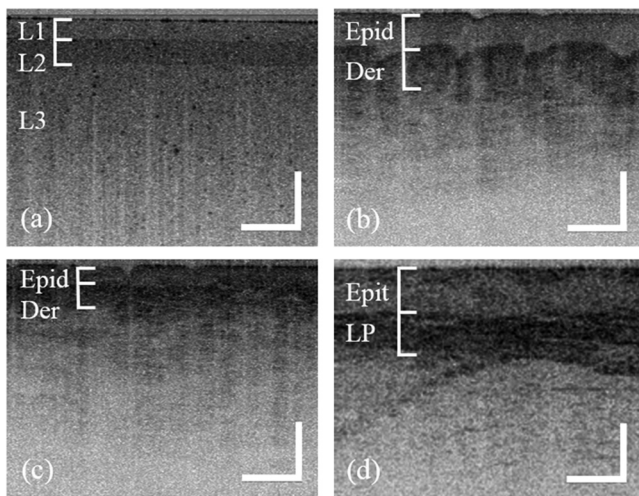spectively. 1 w/v% nigrosin/EtOH concentration was 2.0 μL/g in all layers. The comparative images show OCT B-scans from a normal volunteer of the (b) fingertip showing the epidermis (Epid) and dermis (Der), (c) wrist showing the epidermis (Epid) and dermis (Der), (d) oral mucosa showing the epithelium (Epit) and lamina propria (LP) Scale bars represents 500 μm.

Figure 9 represents an OCT B-scan comparison between multilayered phantoms and several types of human epithelium from a normal volunteer (fingertip epithelium, wrist epithelium, and oral mucosa).

4 Discussion

4.1 PDMS as a Substrate Material

We have demonstrated a reproducible method for creating thin PDMS-based phantoms with tunable thicknesses and optical properties (reduced scattering and absorption coefficients).[1,3,9–12,15] PDMS, a silicone-based polymer, was chosen as the substrate material due to its relatively long optical stability when compared to other commonly used substrates.[1,9] Bruin et al. demonstrated that the optical properties of PDMS-based

phantoms using TiO$_2$ as a scattering agent remained stable over a 6-month testing period.[1] Pogue and Patterson report that silicone-based phantoms with TiO$_2$ and various inks should have an optical stability of at least 1 year.[9] Furthermore, PDMS is optically clear, easily moldable, and has a comparable refractive index (1.4) to human tissue.[1,3,9]

4.2 Spin Coating to Produce Individual Thin Layers

We demonstrated an ability to create both thin phantom layers (between 115 and 880 μm) and thick phantom layers (approximately 2.5-cm thick). Thick phantoms could be made at other thicknesses as well by varying the volume dispensed into the ARE-100 conditioning mixer cup (Intertronics, UK) mold.

To create thin phantom layers, a spin coating technique was used to spin partially cured PDMS down to reproducible thicknesses as shown in Fig. 1.[15,16] Koschwanez et al. have previously outlined a spin coating technique to create multilayered PDMS phantoms by spinning uncured PDMS over an already cured layer. However, their thin phantoms ranged between 2 and 30 μm, much thinner than our intended range (100 to 300 μm) for mimicking epithelial tissue thickness.[13,16–18] Furthermore, our method allowed for thin layers to be used interchangeably and nonpermanently to rapidly test multiple configurations. In our studies, the relationship between the maximum 20-s spin speed of the spin coater and the resulting thicknesses of cured, individual PDMS layers containing varying amounts of TiO$_2$ and 1% w/v nigrosin/EtOH can be seen in Fig. 1. Spin speeds of 100 rpm produced phantoms with an average thickness of 880 μm and a standard deviation of 34 μm. Spin speeds of 1000 μm produced phantoms with an average thickness of 115 μm and standard deviation of 4 μm. As the spin speed increased, the thickness decreased and the standard deviation tended to decrease. For researchers interested in using this technique, the following inverse equation, based on data presented here, can be used as a guideline to estimate the necessary spin speed (rpm) given a desired thickness with relative accuracy,

$$s = 115{,}900 \cdot (t^{-0.9985}) - 15.09, \qquad (1)$$

where t is the desired thickness (μm) and s is the resulting spin speed (rpm). The R^2 value for this equation is 0.988 for the data presented in this manuscript. This equation was generated by the MATLAB curve fitting toolbox using a two-term power model.

One consideration when using this spin coating technique is the potential nonuniformity of the absorbing and scattering agents within the PDMS material. Heterogeneities in these materials may result in increasing radial distances due to the rotational acceleration of the spin coater.[3] This may also mean that thin phantoms of identical concentrations of optical agents but different thicknesses may have slightly different optical properties. Since SFDI required thick phantoms (>2.5 cm) for characterization, the optical properties of thin layers were not explicitly measured.[21] However, from data presented in Figs. 7 and 8, we are reasonably confident that thin layers have bulk scattering and absorbing properties comparable to the thicker layers characterized by SFDI. To definitively validate the thin layer uniformity, methods capable of characterizing the optical properties of thin layers, such as integrating spheres and inverse adding-doubling methods, must be further explored.[24,25] Another limitation to this procedure was creating phantoms with a lower limit of approximately 115 μm. While thinner layers could potentially be produced using our spin coating technique, such thin layers were

increasingly difficult to work with by hand and could no longer be considered interchangeable with regard to creating multilayered phantoms. Therefore, applications in need of phantoms thinner than 115 μm, such as retinal imaging, may benefit from other spin coating techniques such as those presented by Bae et al. or Koschwanez et al. that can produce much thinner layers.[15,16,19]

4.3 Alcohol-Soluble Nigrosin as an Absorbing Agent

The absorption coefficient (μ_a) of PDMS phantoms was manipulated by using alcohol–soluble nigrosin as the absorbing agent.[3,12] A 1% w/v solution of nigrosin/ethanol was prepared and added to phantoms at increasing concentrations as seen in Fig. 5. Figure 6 shows that μ_a was independent of the TiO$_2$ concentration. However, μ_a was shown to be wavelength dependent when using 1% w/v nigrosin/EtOH for the absorbing agent. This can be seen in Fig. 5 in the difference between the best fit curves for the 591 nm (dashed) and 851 nm (dotted) wavelengths, respectively. As the wavelength increased, μ_a tended to decrease. This observation is comparable to results on similar phantoms created by Saager et al.[3] In addition, μ_a was strongly dependent on the concentration of 1% w/v nigrosin/EtOH, as expected. Figure 5 shows that a more linear region exists between 1% w/v nigrosin/EtOH concentrations from 0 to 7 μL/g PDMS elastomer base, corresponding to μ_a values between approximately 0 and $0.9 - 1.2$ cm^{-1} depending on the measured wavelengths. Increases in μ_a began to level off for 1% w/v nigrosin/EtOH concentrations between 7 to 40 μL/g PDMS elastomer base, corresponding to μ_a values between approximately 0.9–1.2 and 1.5 cm^{-1}.

Just as in the case of the previous thickness-spin speed relationship [Eq. (1)], a useful inverse equation would be one that estimates the necessary concentration of 1% w/v nigrosin/EtOH in PDMS given a desired μ_a. Because μ_a was shown to be dependent on both absorbing concentration and wavelength, a simple inverse equation was not found. Instead, the relationship between absorbing agent concentration and the desired μ_a was modeled by a piecewise function for each of the six studied wavelengths (591, 631, 659, 691, 731, and 851 nm). This set of equations, generated by the MATLAB curve-fitting toolbox, was used to create the lookup tables found in the Appendix. However, it should be noted that these equations and the corresponding lookup tables generated from our limited sample size of 16 PDMS-based phantoms (Table 1), should just be used as guidelines. Exact μ_a values cannot be accurately predicted due to our lack of extensive validation testing; therefore, optical properties should always be independently validated.

One of the major drawbacks to using alcohol–soluble nigrosin as the absorber was its hydrophilic nature. The alcohol–soluble nigrosin did not mix easily with the silicone base material used to produce the PDMS. To account for this, Bisaillon et al. and Bruin et al. suggest mixing hexane with PDMS.[1,26] However, Koschwanez et al. suggested that adding hexane swells the PDMS substrate, and instead mixed tert-butyl alcohol with PDMS.[16] Using a certain percent tert-butyl alcohol within the PDMS substrate may aid in more efficient mixing of the alcohol–soluble nigrosin and should be explored in future studies. If this is to be done, however, new thickness-spin speed curves (see Fig. 1) would need to be generated between 100 and 1000 rpm for tert-butyl alcohol infused PDMS.[16] However, our described procedure accounted for mixing difficulties by thoroughly mixing 1% w/v nigrosin/EtOH in PDMS with a sonicator, vortex mixer, and an ARE-100 conditioning

mixer. Another limitation of the phantoms presented here was a characteristic peak in absorption in the 870 to 930 nm range when using nigrosin-silicone-based tissue phantoms.[3] Because our SFDI analysis only covered a wavelength range up to 851 nm, this phenomenon was not observed. Therefore, for our purposes, the procedure presented here to manipulate μ_a using alcohol–soluble nigrosin is sufficient. Finally, other absorbing agents such as whole blood, inks, dyes, or fluorophores may be investigated either as a single absorber or in combination with each other in the outlined procedure for phantom construction.[3,9]

4.4 Titanium Dioxide as a Scattering Agent

The reduced scattering coefficient (μ_s') of PDMS phantoms was manipulated by using TiO$_2$ as the scattering agent.[3] The μ_s' of PDMS phantoms was known to be dependent on the TiO$_2$ concentration (Fig. 3), wavelength (Fig. 3), and 1% w/v nigrosin/ EtOH concentration (Fig. 4). The dependence of μ_s' on the scattering agent concentration and wavelength has been demonstrated in previous phantom studies.[1,3] Depending on the wavelength, Fig. 3 shows that phantoms were produced with reduced scattering coefficients between approximately 1 and 20 cm^{-1}. However, Fig. 4 shows that as the 1% w/v nigrosin/EtOH concentration increased, μ_s' decreased in phantoms with identical concentrations of TiO$_2$ (Phantoms #1, 9–15 in Table 1). Furthermore, the decline of μ_s' due to the increased concentration of 1% w/v nigrosin/EtOH was greater at lower wavelengths (591 and 621 nm) when compared to higher wavelengths (731 and 851 nm). Furthermore, in Fig. 4, once a certain concentration of 1% w/v nigrosin/EtOH was reached (around 7 μL/g), further changes in wavelength and concentration did not affect μ_s'.

The linear relationship between μ_s' and the absorbing agent concentration over the tested wavelengths (Fig. 4) roughly implies that there may exist an empirically determined correction factor that could account for all variables (TiO$_2$ concentration, wavelength, and 1% w/v nigrosin/EtOH concentration) that affect μ_s'. Thus, given a desired wavelength, μ_a, and μ_s', the necessary TiO$_2$ concentration was analytically determined. Therefore, for researchers interested in manipulating μ_s' within PDMS phantoms, the provided lookup tables can predict TiO$_2$ concentration based on data presented in this paper. Of note, however, in Fig. 4, the phenomenon that increasing 1% w/v nigrosin/EtOH concentration reduced μ_s' was only observed in phantoms with minimal TiO$_2$ concentration (0.001 g TiO$_2$/g PDMS elastomer base). Further studies will need to be completed to validate the lookup tables presented here and determine whether this phenomenon is prevalent in phantoms with much higher TiO$_2$ concentrations, such as 0.007 or 0.008 g TiO$_2$/g PDMS elastomer base. It should also be noted that the lookup tables assume a linear relationship in μ_s' and TiO$_2$ concentration beyond the tested limits (0.001-0.008 g/g). Further SFDI analysis will be needed to validate these values within the lookup table.

Finally, it is possible to expand this approach by using scattering agents other than TiO$_2$. Scattering materials, such as polystyrene beads, silicon dioxide, aluminum oxide powders, or other types of microspheres, have been successfully demonstrated by other investigators and could potentially be applied using our spin coater approach.[1,9,27,28]

4.5 Multilayered Phantoms to Simulate Heterogeneities

Generally, the purpose of multilayered phantoms is to introduce geometrical and optical heterogeneities in phantoms to simulate

the layered structure of epithelial tissue.[1,9] A multilayered phantom (Table 2, Phantom #18) with two thin layers (200 μm) was compared to a control phantom (Table 2, Phantom #17) with identical concentrations of optical agents. The μ_s' and μ_a for the two phantoms were compared in Figs. 7 and 8. Only slight differences were present between the two phantoms across the six measured wavelengths. Figure 7, comparing μ_s', shows an average aggregate error of 7.7%. Figure 8, comparing μ_a, shows an average aggregate error 10.9%. We believe these differences were due to random error in dispensing the precise amounts of TiO$_2$ and 1% w/v nigrosin/EtOH solution rather than being due to air pockets between the layers. This assumption was further validated in Fig. 9, which compares multilayered phantoms to human epithelium using an OCT B-scan technique. OCT instrumentation, operating at 1325 nm (outside the wavelength range of our SFDI equipment), was used for comparative purposes and was not meant to validate the optical properties of phantoms. The multilayered phantom (Fig. 9) shows no visible air pockets between adjacent layers. These validations give us good reason to believe that creating PDMS-based multilayered phantoms using our procedure can serve as appropriate models of various epithelia. In addition to providing evidence for the absence of air pockets, the B-scans in Fig. 9 were used for visually comparing thicknesses of the phantoms to several types of epithelium.[23]

The comparative images shown in Fig. 9 as well as the data from Fig. 1 show that the thickness of individual PDMS layers accurately modeled the thickness of several types of human epithelia (skin from the finger or wrist and oral mucosa). In addition, we believe that the phantom procedure presented here could potentially model the thickness of other epithelial tissue types, such as the tongue and gingivae (100 to 200-μm thick, cervical epithelium (180-μm thick), and esophageal epithelium (250-μm thick).[13,17,18]

To design these phantoms, lookup tables have been provided in the Appendix to guide researchers in selecting the appropriate concentrations of scattering and absorbing agents (TiO$_2$ and 1% w/v nigrosin/EtOH). Thick or thin (between 115 and 880 μm) phantoms can be created by either directly molding uncured PDMS or by using the described spin coating technique.

Equation (1) provides guidance in selecting an appropriate spin speed based on a desired phantom layer thickness. Thick and thin layers can be combined to form multilayered phantoms to simulate the optical heterogeneities seen in tissue (Figs. 7–9). In addition, individual thin layers may be used interchangeably to rapidly test multiple configurations.[3] These PDMS-based tissue-simulating phantoms may be used by researchers as optically stable calibration devices for various optical imaging techniques including, but not limited to, OCT, diffuse optical spectroscopic imaging, endoscopy, or microendoscopy.[1–4,9,23] Using the provided lookup tables, these phantoms have the potential to mimic the optical properties of common types of epithelia including breast, skin, colon, oral, cervical, esophagus, etc.[11,13,17,18]

Appendix: Lookup Tables for Optical Properties of Poly(dimethylsiloxane)-Based Phantoms

Tables 4–9 are lookup tables that can be used as guidelines to determine approximate concentrations of the studied absorbing agent (1% w/v nigrosin/EtOH) and scattering agent (titanium dioxide) given a desired absorption coefficient (μ_a) and reduced scattering coefficient (μ_s') at a specific wavelength when designing PDMS-based tissue-simulating phantoms. Six lookup tables are included, corresponding to the six wavelengths (591, 631, 659, 691, 731, and 851 nm) used in this study. It should be noted that individual concentrations listed in this table were not explicitly measured. Instead, the individual concentrations listed here were acquired based on empirical mathematical models fitting the presented data. While the tables do fit the presented data, extensive validation of these tables was not performed. Therefore, optical properties should always be independently validated.

To use these lookup tables, first choose a desired μ_a to obtain the correct concentration of 1% w/v nigrosin/EtOH in the PDMS elastomer base (μL/g). Then, choose a desired μ_s' and line up this row with the column corresponding to the chosen μ_a to obtain the correct concentration of TiO$_2$ in PDMS elastomer base (g/g).

Table 4 Lookup table to determine the required concentrations of absorbing and scattering agents from desired absorption and reduced scattering coefficients at 591 nm.

	Absorption coefficient μ_a (cm^{-1})													
	Concentration of 1% w/v nigrosin/EtOH to PDMS elastomer base (μL/g)													
	0.1	*0.2*	*0.3*	*0.4*	*0.5*	*0.6*	*0.7*	*0.8*	*0.9*	*1.0*	*1.1*	*1.2*	*1.3*	*1.4*
	1.0	1.3	1.7	2.1	2.4	2.8	3.1	3.5	4.1	4.9	5.8	6.6	7.1	13.9
	Reduced scattering coefficient μ_s' (cm^{-1})													
	Concentration of titanium dioxide to PDMS elastomer base (g/g) $\times 10^{-3}$													
1	0.1	0.1	0.1	0.2	0.2	0.2	0.2	0.3	0.3	0.5	0.6	0.9	1.1	1.1
2	0.5	0.5	0.6	0.6	0.7	0.7	0.8	0.9	1.0	1.2	1.6	2.2	2.6	2.6
3	0.9	1.0	1.0	1.1	1.2	1.3	1.3	1.4	1.7	2.0	2.6	3.4	4.0	4.0
4	1.3	1.4	1.5	1.6	1.7	1.8	1.9	2.0	2.3	2.8	3.5	4.7	5.5	5.5
5	1.7	1.8	1.9	2.0	2.2	2.3	2.4	2.6	3.0	3.6	4.5	5.9	7.0	7.0

Table 4 (*Continued*).

						Absorption coefficient μ_a (cm^{-1})							
					Concentration of 1% w/v nigrosin/EtOH to PDMS elastomer base (μL/g)								
6	2.2	2.3	2.4	2.5	2.7	2.8	3.0	3.2	3.6	4.4	5.4	7.2	8.4	8.4
7	2.6	2.7	2.8	3.0	3.2	3.3	3.5	3.8	4.3	5.1	6.4	8.4	9.9	9.9
8	3.0	3.1	3.3	3.5	3.6	3.9	4.1	4.4	4.9	5.9	7.4	9.7	11.3	11.3
9	3.4	3.5	3.7	3.9	4.1	4.4	4.7	5.0	5.6	6.7	8.3	10.9	12.8	12.8
10	3.8	4.0	4.2	4.4	4.6	4.9	5.2	5.5	6.2	7.5	9.3	12.2	14.2	14.2
11	4.2	4.4	4.6	4.9	5.1	5.4	5.8	6.1	6.9	8.2	10.2	13.4	15.7	15.7
12	4.6	4.8	5.1	5.3	5.6	5.9	6.3	6.7	7.5	9.0	11.2	14.7	17.1	17.1
13	5.0	5.3	5.5	5.8	6.1	6.5	6.9	7.3	8.2	9.8	12.1	15.9	18.6	18.6
14	5.4	5.7	6.0	6.3	6.6	7.0	7.4	7.9	8.8	10.6	13.1	17.2	20.0	20.0
15	5.8	6.1	6.4	6.7	7.1	7.5	8.0	8.5	9.5	11.3	14.1	18.4	21.5	21.5
16	6.3	6.5	6.9	7.2	7.6	8.0	8.5	9.0	10.2	12.1	15.0	19.7	22.9	22.9
17	6.7	7.0	7.3	7.7	8.1	8.6	9.1	9.6	10.8	12.9	16.0	20.9	24.4	24.4
18	7.1	7.4	7.8	8.2	8.6	9.1	9.6	10.2	11.5	13.7	16.9	22.2	25.8	25.8
19	7.5	7.8	8.2	8.6	9.1	9.6	10.2	10.8	12.1	14.5	17.9	23.4	27.3	27.3
20	7.9	8.3	8.7	9.1	9.6	10.1	10.7	11.4	12.8	15.2	18.8	24.7	28.7	28.7

Table 5 Lookup table to determine the required concentrations of absorbing and scattering agents from desired absorption and reduced scattering coefficients at 631 nm.

						Absorption coefficient μ_a (cm^{-1})							
					Concentration of 1% w/v nigrosin/EtOH to PDMS elastomer base (μL/g)								
0.1	*0.2*	*0.3*	*0.4*	*0.5*	*0.6*	*0.7*	*0.8*	*0.9*	*1.0*	*1.1*	*1.2*	*1.3*	*1.4*
1.0	1.4	1.7	2.1	2.5	2.9	3.2	3.6	4.2	5.1	5.9	6.8	7.3	14.5

						Reduced scattering coefficient μ_s' (cm^{-1})							
					Concentration of titanium dioxide to PDMS elastomer base (g/g) $\times 10^{-3}$								
1	0.2	0.2	0.2	0.2	0.3	0.3	0.3	0.4	0.4	0.6	0.7	1.0	1.1	1.1
2	0.7	0.7	0.7	0.8	0.8	0.9	1.0	1.0	1.2	1.4	1.8	2.3	2.5	2.5
3	1.1	1.2	1.3	1.3	1.4	1.5	1.6	1.7	1.9	2.3	2.8	3.6	3.9	3.9
4	1.6	1.7	1.8	1.9	2.0	2.1	2.2	2.4	2.6	3.1	3.8	4.9	5.3	5.3
5	2.1	2.2	2.3	2.4	2.5	2.7	2.8	3.0	3.4	4.0	4.9	6.2	6.7	6.7
6	2.5	2.7	2.8	2.9	3.1	3.3	3.5	3.7	4.1	4.8	5.9	7.5	8.1	8.1
7	3.0	3.1	3.3	3.5	3.7	3.9	4.1	4.3	4.8	5.7	6.9	8.8	9.5	9.5
8	3.5	3.6	3.8	4.0	4.2	4.4	4.7	5.0	5.6	6.6	8.0	10.1	10.9	10.9
9	3.9	4.1	4.3	4.5	4.8	5.0	5.3	5.7	6.3	7.4	9.0	11.4	12.3	12.3
10	4.4	4.6	4.8	5.1	5.3	5.6	6.0	6.3	7.0	8.3	10.0	12.7	13.7	13.7
11	4.9	5.1	5.3	5.6	5.9	6.2	6.6	7.0	7.8	9.1	11.1	14.0	15.1	15.1
12	5.4	5.6	5.9	6.1	6.5	6.8	7.2	7.6	8.5	10.0	12.1	15.3	16.4	16.4
13	5.8	6.1	6.4	6.7	7.0	7.4	7.8	8.3	9.2	10.8	13.1	16.6	17.8	17.8

Table 5 (*Continued*).

	Absorption coefficient μ_a (cm^{-1})													
	Concentration of 1% w/v nigrosin/EtOH to PDMS elastomer base (μL/g)													
14	6.3	6.6	6.9	7.2	7.6	8.0	8.4	9.0	10.0	11.7	14.1	17.9	19.2	19.2
15	6.8	7.1	7.4	7.8	8.2	8.6	9.1	9.6	10.7	12.6	15.2	19.1	20.6	20.6
16	7.2	7.6	7.9	8.3	8.7	9.2	9.7	10.3	11.4	13.4	16.2	20.4	22.0	22.0
17	7.7	8.0	8.4	8.8	9.3	9.8	10.3	10.9	12.2	14.3	17.2	21.7	23.4	23.4
18	8.2	8.5	8.9	9.4	9.8	10.4	10.9	11.6	12.9	15.1	18.3	23.0	24.8	24.8
19	8.6	9.0	9.4	9.9	10.4	11.0	11.6	12.3	13.6	16.0	19.3	24.3	26.2	26.2
20	9.1	9.5	10.0	10.4	11.0	11.5	12.2	12.9	14.4	16.8	20.3	25.6	27.6	27.6

Table 6 Lookup table to determine the required concentrations of absorbing and scattering agents from desired absorption and reduced scattering coefficients at 659 nm.

	Absorption coefficient μ_a (cm^{-1})													
	Concentration of 1% w/v nigrosin/EtOH to PDMS elastomer base (μL/g)													
	0.1	*0.2*	*0.3*	*0.4*	*0.5*	*0.6*	*0.7*	*0.8*	*0.9*	*1.0*	*1.1*	*1.2*	*1.3*	*1.4*
	1.0	1.4	1.8	2.2	2.6	3.0	3.3	3.7	4.4	5.2	6.0	6.8	7.5	12.6

	Reduced scattering coefficient μ_s' (cm^{-1})													
	Concentration of titanium dioxide to PDMS elastomer base (g/g) $\times 10^{-3}$													
1	0.3	0.3	0.3	0.3	0.4	0.4	0.4	0.5	0.5	0.7	0.8	1.0	1.1	1.1
2	0.8	0.8	0.9	0.9	1.0	1.1	1.1	1.2	1.4	1.6	1.9	2.3	2.4	2.4
3	1.3	1.4	1.5	1.5	1.6	1.7	1.8	1.9	2.2	2.5	2.9	3.6	3.8	3.8
4	1.8	1.9	2.0	2.1	2.2	2.4	2.5	2.6	3.0	3.4	4.0	4.8	5.1	5.1
5	2.4	2.5	2.6	2.7	2.9	3.0	3.2	3.4	3.8	4.3	5.1	6.1	6.5	6.5
6	2.9	3.0	3.2	3.3	3.5	3.7	3.9	4.1	4.6	5.3	6.1	7.4	7.8	7.8
7	3.4	3.6	3.7	3.9	4.1	4.3	4.6	4.8	5.4	6.2	7.2	8.7	9.2	9.2
8	3.9	4.1	4.3	4.5	4.7	5.0	5.3	5.6	6.2	7.1	8.3	9.9	10.5	10.5
9	4.5	4.7	4.9	5.1	5.4	5.6	5.9	6.3	7.0	8.0	9.4	11.2	11.9	11.9
10	5.0	5.2	5.4	5.7	6.0	6.3	6.6	7.0	7.8	8.9	10.4	12.5	13.2	13.2
11	5.5	5.8	6.0	6.3	6.6	6.9	7.3	7.7	8.6	9.8	11.5	13.8	14.6	14.6
12	6.0	6.3	6.6	6.9	7.2	7.6	8.0	8.5	9.4	10.8	12.6	15.0	15.9	15.9
13	6.6	6.8	7.2	7.5	7.9	8.3	8.7	9.2	10.2	11.7	13.6	16.3	17.3	17.3
14	7.1	7.4	7.7	8.1	8.5	8.9	9.4	9.9	11.0	12.6	14.7	17.6	18.6	18.6
15	7.6	7.9	8.3	8.7	9.1	9.6	10.1	10.6	11.8	13.5	15.8	18.9	20.0	20.0
16	8.1	8.5	8.9	9.3	9.7	10.2	10.8	11.4	12.6	14.4	16.8	20.1	21.3	21.3
17	8.7	9.0	9.4	9.9	10.3	10.9	11.5	12.1	13.4	15.4	17.9	21.4	22.7	22.7
18	9.2	9.6	10.0	10.5	11.0	11.5	12.1	12.8	14.2	16.3	19.0	22.7	24.0	24.0
19	9.7	10.1	10.6	11.1	11.6	12.2	12.8	13.6	15.0	17.2	20.0	24.0	25.4	25.4
20	10.2	10.7	11.1	11.7	12.2	12.8	13.5	14.3	15.9	18.1	21.1	25.2	26.7	26.7

Table 7 Lookup table to determine the required concentrations of absorbing and scattering agents from desired absorption and reduced scattering coefficients at 691 nm.

Absorption coefficient μ_a (cm^{-1})													
Concentration of 1% w/v nigrosin/EtOH to PDMS elastomer base (μL/g)													
0.1	0.2	0.3	0.4	0.5	0.6	0.7	0.8	0.9	1.0	1.1	1.2	1.3	1.4
1.0	1.4	1.8	2.3	2.7	3.1	3.5	3.9	4.7	5.4	6.1	6.8	7.3	9.1

Reduced scattering coefficient μ_s' (cm^{-1})														
Concentration of titanium dioxide to PDMS elastomer base (g/g) $\times 10^{-3}$														
1	0.4	0.4	0.5	0.5	0.5	0.5	0.6	0.6	0.7	0.8	0.9	1.0	1.1	1.1
2	1.0	1.0	1.1	1.1	1.2	1.2	1.3	1.4	1.5	1.7	1.9	2.2	2.3	2.3
3	1.6	1.6	1.7	1.8	1.9	1.9	2.0	2.2	2.4	2.6	3.0	3.4	3.5	3.5
4	2.1	2.2	2.3	2.4	2.5	2.6	2.8	2.9	3.2	3.6	4.0	4.6	4.7	4.7
5	2.7	2.8	2.9	3.0	3.2	3.3	3.5	3.7	4.1	4.5	5.0	5.7	5.9	5.9
6	3.3	3.4	3.5	3.7	3.9	4.0	4.2	4.5	4.9	5.4	6.1	6.9	7.2	7.2
7	3.8	4.0	4.1	4.3	4.5	4.7	5.0	5.2	5.7	6.4	7.1	8.1	8.4	8.4
8	4.4	4.6	4.8	5.0	5.2	5.4	5.7	6.0	6.6	7.3	8.2	9.3	9.6	9.6
9	5.0	5.2	5.4	5.6	5.9	6.1	6.4	6.8	7.4	8.2	9.2	10.4	10.8	10.8
10	5.5	5.7	6.0	6.2	6.5	6.8	7.2	7.5	8.3	9.2	10.2	11.6	12.0	12.0
11	6.1	6.3	6.6	6.9	7.2	7.5	7.9	8.3	9.1	10.1	11.3	12.8	13.2	13.2
12	6.7	6.9	7.2	7.5	7.9	8.2	8.6	9.1	10.0	11.0	12.3	14.0	14.5	14.5
13	7.2	7.5	7.8	8.2	8.5	8.9	9.4	9.8	10.8	12.0	13.4	15.2	15.7	15.7
14	7.8	8.1	8.4	8.8	9.2	9.6	10.1	10.6	11.6	12.9	14.4	16.3	16.9	16.9
15	8.4	8.7	9.0	9.4	9.9	10.3	10.8	11.4	12.5	13.8	15.4	17.5	18.1	18.1
16	8.9	9.3	9.7	10.1	10.5	11.0	11.6	12.1	13.3	14.7	16.5	18.7	19.3	19.3
17	9.5	9.9	10.3	10.7	11.2	11.7	12.3	12.9	14.2	15.7	17.5	19.9	20.6	20.6
18	10.1	10.5	10.9	11.4	11.9	12.4	13.0	13.7	15.0	16.6	18.6	21.0	21.8	21.8
19	10.6	11.0	11.5	12.0	12.5	13.1	13.7	14.5	15.9	17.5	19.6	22.2	23.0	23.0
20	11.2	11.6	12.1	12.6	13.2	13.8	14.5	15.2	16.7	18.5	20.6	23.4	24.2	24.2

Table 8 Lookup table to determine the required concentrations of absorbing and scattering agents from desired absorption and reduced scattering coefficients at 731 nm.

	Absorption coefficient μ_a (cm^{-1})													
	Concentration of 1% w/v nigrosin/EtOH to PDMS elastomer base (μL/g)													
	0.1	0.2	0.3	0.4	0.5	0.6	0.7	0.8	0.9	1.0	1.1	1.2	1.3	1.4
	1.0	1.5	1.9	2.4	2.8	3.3	3.8	4.3	5.1	5.8	6.5	7.3	9.3	17.3
	Reduced scattering coefficient μ_s' (cm^{-1})													
	Concentration of titanium dioxide to PDMS elastomer base (g/g) $\times 10^{-3}$													
1	0.5	0.5	0.5	0.6	0.6	0.6	0.7	0.7	0.8	0.9	1.0	1.0	1.0	1.0
2	1.1	1.2	1.2	1.3	1.3	1.4	1.4	1.5	1.7	1.8	2.0	2.2	2.2	2.2
3	1.7	1.8	1.9	1.9	2.0	2.1	2.2	2.4	2.6	2.8	3.1	3.4	3.4	3.4
4	2.3	2.4	2.5	2.6	2.7	2.9	3.0	3.2	3.5	3.8	4.2	4.5	4.5	4.5
5	2.9	3.1	3.2	3.3	3.5	3.6	3.8	4.0	4.4	4.8	5.3	5.7	5.7	5.7
6	3.6	3.7	3.8	4.0	4.2	4.4	4.6	4.9	5.3	5.8	6.4	6.8	6.8	6.8
7	4.2	4.3	4.5	4.7	4.9	5.1	5.4	5.7	6.2	6.8	7.5	8.0	8.0	8.0
8	4.8	5.0	5.2	5.4	5.6	5.9	6.1	6.5	7.1	7.7	8.5	9.2	9.2	9.2
9	5.4	5.6	5.8	6.1	6.3	6.6	6.9	7.4	8.0	8.7	9.6	10.3	10.3	10.3
10	6.0	6.2	6.5	6.8	7.0	7.4	7.7	8.2	8.9	9.7	10.7	11.5	11.5	11.5
11	6.6	6.9	7.1	7.4	7.8	8.1	8.5	9.0	9.8	10.7	11.8	12.6	12.6	12.6
12	7.2	7.5	7.8	8.1	8.5	8.9	9.3	9.9	10.7	11.7	12.9	13.8	13.8	13.8
13	7.9	8.1	8.5	8.8	9.2	9.6	10.1	10.7	11.6	12.7	13.9	15.0	15.0	15.0
14	8.5	8.8	9.1	9.5	9.9	10.4	10.8	11.5	12.5	13.6	15.0	16.1	16.1	16.1
15	9.1	9.4	9.8	10.2	10.6	11.1	11.6	12.3	13.4	14.6	16.1	17.3	17.3	17.3
16	9.7	10.1	10.5	10.9	11.3	11.9	12.4	13.2	14.3	15.6	17.2	18.4	18.4	18.4
17	10.3	10.7	11.1	11.6	12.1	12.6	13.2	14.0	15.2	16.6	18.3	19.6	19.6	19.6
18	10.9	11.3	11.8	12.3	12.8	13.3	14.0	14.8	16.1	17.6	19.4	20.8	20.8	20.8
19	11.5	12.0	12.4	12.9	13.5	14.1	14.8	15.7	17.0	18.6	20.4	21.9	21.9	21.9
20	12.1	12.6	13.1	13.6	14.2	14.8	15.5	16.5	17.9	19.5	21.5	23.1	23.1	23.1

Table 9 Lookup table to determine the required concentrations of absorbing and scattering agents from desired absorption and reduced scattering coefficients at 851 nm.

	Absorption coefficient μ_a (cm^{-1})													
	Concentration of 1% w/v nigrosin/EtOH to PDMS elastomer base (μL/g)													
	0.1	*0.2*	*0.3*	*0.4*	*0.5*	*0.6*	*0.7*	*0.8*	*0.9*	*1.0*	*1.1*	*1.2*	*1.3*	*1.4*
	1.0	1.7	2.4	3.1	3.8	4.4	5.2	5.9	6.7	7.7	9.6	12.9	18.4	27.4

	Reduced scattering coefficient μ_s' (cm^{-1})													
	Concentration of titanium dioxide to PDMS elastomer base (g/g) $\times 10^{-3}$													
1	0.6	0.6	0.7	0.7	0.7	0.7	0.8	0.8	0.8	0.8	0.8	0.8	0.8	0.8
2	1.4	1.4	1.4	1.5	1.5	1.6	1.6	1.7	1.8	1.8	1.8	1.8	1.8	1.8
3	2.1	2.1	2.2	2.3	2.4	2.4	2.5	2.6	2.7	2.8	2.8	2.8	2.8	2.8
4	2.8	2.9	3.0	3.1	3.2	3.3	3.4	3.5	3.7	3.7	3.7	3.7	3.7	3.7
5	3.6	3.7	3.8	3.9	4.0	4.1	4.3	4.4	4.6	4.7	4.7	4.7	4.7	4.7
6	4.3	4.4	4.5	4.7	4.8	5.0	5.2	5.4	5.6	5.7	5.7	5.7	5.7	5.7
7	5.0	5.2	5.3	5.5	5.7	5.8	6.0	6.3	6.5	6.6	6.6	6.6	6.6	6.6
8	5.8	5.9	6.1	6.3	6.5	6.7	6.9	7.2	7.5	7.6	7.6	7.6	7.6	7.6
9	6.5	6.7	6.9	7.1	7.3	7.5	7.8	8.1	8.4	8.6	8.6	8.6	8.6	8.6
10	7.2	7.4	7.7	7.9	8.1	8.4	8.7	9.0	9.4	9.5	9.5	9.5	9.5	9.5
11	8.0	8.2	8.4	8.7	9.0	9.2	9.6	9.9	10.3	10.5	10.5	10.5	10.5	10.5
12	8.7	9.0	9.2	9.5	9.8	10.1	10.4	10.8	11.3	11.4	11.4	11.4	11.4	11.4
13	9.4	9.7	10.0	10.3	10.6	10.9	11.3	11.7	12.2	12.4	12.4	12.4	12.4	12.4
14	10.2	10.5	10.8	11.1	11.4	11.8	12.2	12.7	13.2	13.4	13.4	13.4	13.4	13.4
15	10.9	11.2	11.6	11.9	12.3	12.6	13.1	13.6	14.1	14.3	14.3	14.3	14.3	14.3
16	11.6	12.0	12.3	12.7	13.1	13.5	14.0	14.5	15.1	15.3	15.3	15.3	15.3	15.3
17	12.4	12.7	13.1	13.5	13.9	14.3	14.8	15.4	16.0	16.3	16.3	16.3	16.3	16.3
18	13.1	13.5	13.9	14.3	14.7	15.2	15.7	16.3	17.0	17.2	17.2	17.2	17.2	17.2
19	13.9	14.2	14.7	15.1	15.6	16.0	16.6	17.2	17.9	18.2	18.2	18.2	18.2	18.2
20	14.6	15.0	15.4	15.9	16.4	16.9	17.5	18.1	18.8	19.2	19.2	19.2	19.2	19.2

References

1. D. M. de Bruin et al., "Optical phantoms of varying geometry based on thin building blocks with controlled optical properties," *J. Biomed. Opt.* **15**(2), 025001 (2010).
2. J. Hwang, J. C. Ramella-Roman, and R. Nordstrom, "Introduction: feature issue on phantoms for the performance evaluation and validation of optical medical imaging devices," *Biomed. Opt. Express* **3**(6), 1399–1403 (2012).
3. R. Saager et al., "Multi-layer silicone phantoms for the evaluation of quantitative optical techniques in skin imaging," *Proc. SPIE* **7567**, 756706 (2010).
4. A. E. Cerussi et al., "Tissue phantoms in multicenter clinical trials for diffuse optical technologies," *Biomed. Opt. Express* **3**(5), 966–971 (2012).
5. A. Agrawal et al., "System-independent assessment of OCT axial resolution with a 'bar chart' phantom," *Proc. SPIE* **7906**, 79060R (2011).
6. R. Y. Gu et al., "Variable-sized bar targets for characterizing three-dimensional resolution in OCT," *Biomed. Opt. Express* **3**(9), 2317–2325 (2012).

7. A. Agrawal et al., "Multilayer thin-film phantoms for axial contrast transfer function measurement in optical coherence tomography," *Biomed. Opt. Express* **4**(7), 1166–1175 (2013).

8. T. Moffitt, Y. C. Chen, and S. A. Prahl, "Preparation and characterization of polyurethane optical phantoms," *J. Biomed. Opt* **11**(4), 041103 (2006).

9. B. W. Pogue and M. S. Patterson, "Review of tissue simulating phantoms for optical spectroscopy, imaging and dosimetry," *J. Biomed. Opt.* **11**(4), 041102 (2006).

10. F. Ayers et al., "Fabrication and characterization of silicone-based tissue phantoms with tunable optical properties in the visible and near infrared domain," *Proc. SPIE* **6870**, 687007 (2008).

11. J. L. Sandell and T. C. Zhu, "A review of in-vivo optical properties of human tissues and its impact on PDT," *J. Biophotonics* **4**(11–12), 773–787 (2011).

12. Q. Liu and N. Ramanujam, "Sequential estimation of optical properties of a two-layered epithelial tissue model from depth-resolved ultraviolet-visible diffuse reflectance spectra," *Appl. Opt.* **45**(19), 4776–4790 (2006).

13. D. Harris and J. R. Robinson, "Drug delivery via the mucous membranes of the oral cavity," *J. Pharm. Sci.* **81**(1), 1–10 (1992).

14. R. C. Chang et al., "Fabrication and characterization of a multilayered optical tissue model with embedded scattering microspheres in polymeric materials," *Biomed. Opt. Express* **3**(6), 1326–1339 (2012).

15. Y. Bae et al., "Fabrication of a thin-layer solid optical tissue phantom by a spin-coating method: pilot study," *J. Biomed. Opt.* **18**(2), 025006 (2013).

16. J. H. Koschwanez et al., "Thin PDMS films using long spin times or tert-butyl alcohol as a solvent," *PLOS One* **4**(2), 4572 (2009).

17. J. V. Guimarães et al., "Thickness of the cervical epithelium of autopsied patients with acquired immunodeficiency syndrome," *Ann. Diagn. Pathol.* **11**(4), 258–261 (2007).

18. L. Rocha et al., "Esophageal epithelium of women with AIDS: thickness and local immunity," *Path. Res. Prac.* **206**(4), 248–252 (2010).

19. J. Baxi et al., "Retina-simulating phantom for optical coherence tomography," *J. Biomed. Opt.* **19**(2), 021106 (2014).

20. S. C. Kanick et al., "Measurement of the reduced scattering coefficient of turbid media using single fiber reflectance spectroscopy: fiber diameter and phase function dependence," *Biomed. Opt. Express* **2**(6), 1687–1702 (2011).

21. D. J. Cuccia et al., "Quantitation and mapping of tissue optical properties using modulated imaging," *J. Biomed. Opt.* **14**(2), 024012 (2009).

22. D. J. Cuccia et al., "Modulated imaging: quantitative analysis and tomography of turbid media in the spatial-frequency domain," *Opt. Lett.* **30**(11), 1354–1356 (2005).

23. L. M. Higgins and M. C. Pierce, "Design and characterization of a hand-held multimodal imaging device for the assessment of oral epithelial lesions," *J. Biomed. Opt.* **19**(8), 086004 (2014).

24. S. A. Prahl, M. J. C. van Gemert, and A. J. Welch, "Determining the optical properties of turbid media by using the adding-doubling method," *Appl. Opt.* **32** (4), 559–568 (1993).

25. J. W. Pickering et al., "Double-integrating-sphere system for measuring the optical properties of tissue," *Appl. Opt.* **32**(4), 399–410 (1993).

26. C. E. Bisaillon et al., "Deformable and durable phantoms with controlled density of scatterers," *Phys. Med. Biol.* **53**(13), N237 (2008).

27. S. C. Kanick et al., "Scattering phase function spectrum makes reflectance spectrum measured from intralipid phantoms and tissue sensitive to the device detection geometry," *Biomed. Opt. Express* **3**(5), 1086–1100 (2012).

28. D. Passos et al., "Tissue phantom for optical diagnostics based on a suspension of microspheres with a fractal size distribution," *J. Biomed. Opt.* **10**(6), 064036 (2005).

Biographies of the authors are not available.